energy&fuels

pubs.acs.org/EF Article

Flexible, Lead-Free Nanogenerators Using Poly(vinylidene fluoride) Nanocomposites

Anupama Gaur, Shivam Tiwari, Chandan Kumar, and Pralay Maiti*

Cite This: *Energy Fuels* 2020, 34, 6239−6244 Read Online

ACCESS | Metrics & More | Article Recommendations | Supporting Information

ABSTRACT: A flexible, lead-free piezoelectric nanogenerator is demonstrated, which produces an electrical signal (voltage) under the application of stress. Barium titanate ($BaTiO_3$) nanoparticles are embedded in the poly(vinylidene fluoride) matrix to prepare the nanocomposite using the solvent-casting method. Different nanocomposites with varying filler content have been prepared. The nanocomposite eliminates the problems of mechanical stability as the polymer provides it better flexibility as compared to the brittle ceramic material. The structural and morphological studies are performed through X-ray diffraction, differential scanning calorimetry, thermogravimetric analysis, polarized optical microscopy, and scanning electron microscopy. In response to mechanical deformation, the voltage is generated, and the output voltage increases with increasing the filler content up to 10 wt %, followed by the reduced electrical signal because of agglomeration of the nanoparticles in the composites. Electric poling is also used to enhance the electrical output from the device. The fabricated device exhibits a very high voltage output of 78 V and 120 $\mu W/cm^2$ power density after poling. The prepared device is also able to harvest different biomechanical energies and also able to charge the capacitor, demonstrating the practical applications of the device. The composite with a suitable filler content can be used in wearable smart clothing and small portable devices.

1. INTRODUCTION

Harvesting energy from ambient mechanical sources has gained promising interest as it can power small electronic devices.[1] In recent years, many attempts have been done for improving the efficiency of energy-harvesting systems. The most common piezoelectric materials used are lead zirconate titanate (PZT) and barium titanate ($BaTiO_3$).[2] However, the ceramics are vulnerable to mechanical and cyclic loading, so we need another flexible alternative like polymers.[3−5] For wearable and implantable devices, it is beneficial that one can harvest the biomechanical energy from different body movements,[6] and polymers are found to be the suitable materials to embed piezoelectric ceramics. Piezoelectric polymers are used in the field of wearable electronics, if they found to be biocompatible. Among these piezoelectric polymers, poly(vinylidene fluoride) is the most widely used polymer.[7,8] The piezoelectric properties of PVDF can be enhanced by preparing the composites using piezo-ceramics as fillers.[9] Many efforts have been done for the development of PVDF−ceramic composites as these composites have better piezoelectric properties of ceramics together with flexibility and scalability because of ease of polymer processing. The ceramics are thermally stable than the polymers. The thermal stability and thermodynamic interactions are important for the phase change to occur or the improvement in mechanical properties. The PVDF−nanoclay hybrid is reported to exhibit the depression in melting point, arising from interactions.[10,11] The hybrid of poly(ethylene terepthalate) with different nanoparticles also shows the changes in the glass transition temperature because of interaction of PET with the nanoclay.[12−14] PZT and barium titanate are the most conventional piezoelectric ceramics, which have high piezoelectric constant, excellent chemical stability, and high temperature stability.[15−17] However, the use of PZT raises concerns because of its harmful effects on human and the environment because of the presence of toxic lead.[18] An alternative to this may be the lead-free polymer-based nanocomposite, which have ease of fabrication, flexibility, light weight, multishape, and adaptability.[19,20] The PVDF−$BaTiO_3$ composite is one of the best alternatives with high energy output. A lot of work has been done with PVDF and $BaTiO_3$ (BT) nanoparticles. Various works has been done with barium titanate and polymer for energy harvesting. Lee et al.[21] prepared uniaxially aligned composite nanofibers of PVDF and BT nanoparticles. The composite nanofibers with 16% BT content showed the output voltage of 0.48 V, corresponding to a 6 mm deflection, which is 1.7 times higher than pure PVDF. Lin et al.[22] prepared a nanogenerator using BT nanorods and poly(dimethyl siloxane) (PDMS) composite, which under a stress of 1 MPa gives a voltage output of 5.5 V and 350 nA. Park et al.[23] prepared the composite of PDMS with the BT nanoparticle and graphitic carbon using spin-casting and performed bending test on the prepared nanogenerator, which gave an output voltage of 6.4 V (peak to peak) with a bending radius of 0.8 cm. The output voltages in most cases are very less for an efficient energy-harvesting material.

Received: April 8, 2020
Revised: April 29, 2020
Published: April 30, 2020

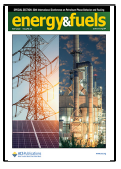

https://dx.doi.org/10.1021/acs.energyfuels.0c01143
Energy Fuels 2020, 34, 6239−6244

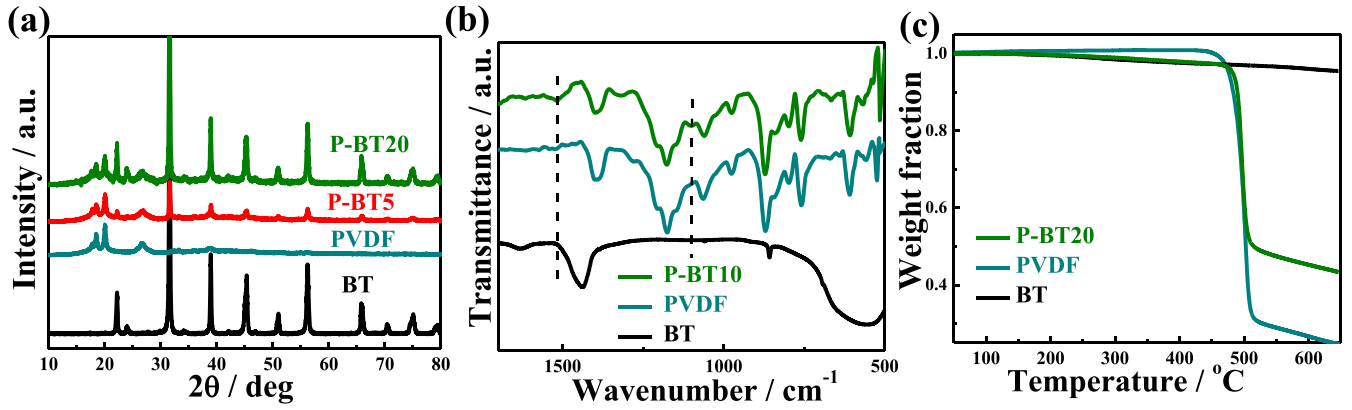

Figure 1. (a) XRD graph for pure PVDF, BT powder, and nanocomposite, FTIR spectra of (b) pure BT powder and (c) pure PVDF and nanocomposite (d), and thermogravimetric analysis plots for pure PVDF, BT, and nanocomposites.

In this study, we report the high-performance, flexible, and lead-free energy-harvesting device, based on $BaTiO_3$ nanoparticles dispersed in the PVDF matrix. Structural and morphological changes in the nanocomposites have been studied in detail. Piezoelectric nanogenerators have been fabricated using these nanocomposites to evaluate the energy-harvesting capability of the material. Poling has been done to improve the charge generation from the device, and the practical applications of the device have been shown from different human motions, capacitor charging, and light-emitting diode (LED) lightning.

2. EXPERIMENTAL SECTION

2.1. Materials. Barium carbonate ($BaCO_3$) and titanium dioxide (TiO_2) are purchased from Hi-media, India. Poly(vinylidene fluoride) (Solvay 6008) is kindly supplied by Austimont, Italy. A common solvent, dimethyl formamide (DMF), is purchased from Hi-media, India, and PDMS for encapsulation is procured from Ellsworth Adhesives, India.

2.2. Sample Preparation. $BaTiO_3$ nanoparticles were prepared through the solid-state method using $BaCO_3$ and TiO_2 powder.[24] For the preparation of the nanocomposites of PVDF and $BaTiO_3$, the $BaTiO_3$ nanoparticles were used as the filler in the PVDF matrix. Different weight ratios of 5, 10, 20, and 40 wt % of filler are used for the preparation of nanocomposites. PVDF is first dissolved in DMF at 60 °C, and $BaTiO_3$ is dispersed in DMF separately using sonication, and then both the solutions were mixed and kept on stirring for 4 h. After complete mixing, the solution was poured in a Petri dish and was kept for drying in an oven, followed by in a vacuum oven. The thin-film samples were prepared using compression molding. Pure barium titanate and polymer is termed as "BT" and "PVDF", respectively. The nanocomposites of PVDF and BT are termed as P-BT5, P-BT10, P-BT20, and P-BT40, where numeric terms indicate the weight fraction of BT in the polymer matrix.

2.3. Device Fabrication. For device fabrication, rectangular samples of 1 × 2 cm^2 area were cut and coated with conducting silver paste at both the sides. After this, the electrodes were attached on both the sides for the measurements and were covered with the polypropylene tape. The complete assembly was then encapsulated with PDMS. In PDMS, the epoxy and hardener were taken in the ratio of 10:1.

2.4. Characterization. X-ray diffraction (XRD) analysis was performed using Rigaku Miniflex 600 operating at 40 kV and 15 mA using Cu Kα radiation (λ = 1.54 Å) at room temperature at a scan rate of 3 °C/min. Fourier Transform Infrared Spectroscopy (FTIR) measurement was performed in the reflectance mode at room temperature from 650 to 4000 cm^{-1} using the Nicolet 5700 instrument, with a resolution of 4 cm^{-1}. Samples of approximately 100 μm thickness were analyzed by polarized optical microscopy (POM): Thin-film samples were analyzed using a polarized optical microscope (Leitz, Biomed) to investigate the surface of the films after their suitable crystallization. Scanning electron microscopy (SEM): the surface morphology of the samples was obtained by using SEM (SUPRA 40, Zeiss). Thin films of the samples were gold-coated by using sputtering before observation in SEM. Differential scanning calorimetry (DSC): the melting temperature of samples was determined using DSC (Mettlers 832). The samples were heated up to 250 °C at a scan rate of 10 °C/min. Voltage measurement was done by using a TektronixTBS-1072B Digital Storage Oscilloscope.

3. RESULTS AND DISCUSSION

3.1. Structure and Morphology. The structure of barium titanate and its nanocomposite with PVDF is studied by using

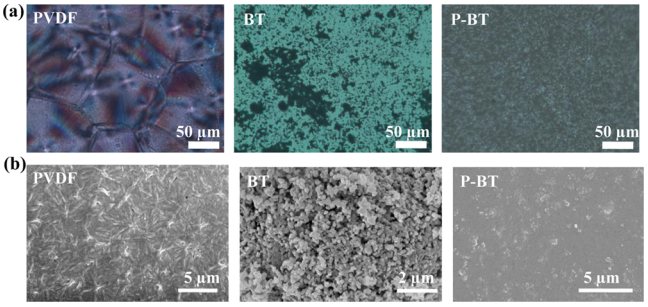

Figure 2. (a) Polarized optical microscopy and (b) scanning electron microscopy images for pure PVDF, BT power, and PVDF-BT nanocomposite.

X-ray diffraction. XRD patterns of pure BT, PVDF, and their nanocomposites are shown in Figure 1a. The barium titanate has its crystalline-phase peaks at $2\theta \approx$ (100) 21.6, (110) 32.5, (200) 45.3, (210) 50.9, (211) 56.2, and (220) 65.8°, confirming the phase-pure BT and following the JCPDS data. The crystalline-phase peaks of barium titanate in the nanocomposite along with its enhanced peak intensity for larger amount of BT nanoparticles confirm the presence of BT in nanocomposites.[25] Pure PVDF crystallizes in the α-form and there is no change of structure in the composite, and the α-phase of PVDF is prominent in the composites. Figure 1b shows the FTIR pattern of BT, PVDF, and nanocomposite (P-BT10). BT nanoparticles exhibit their characteristics peaks at 563, 868, 1433, 1626, and 3434 cm^{-1}. The strong broad band between 563 and 597 cm^{-1} is because of Ti−O stretching mode of $BaTiO_3$[26,27] while the bands at 3434 cm^{-1} correspond

https://dx.doi.org/10.1021/acs.energyfuels.0c01143
Energy Fuels 2020, 34, 6239−6244

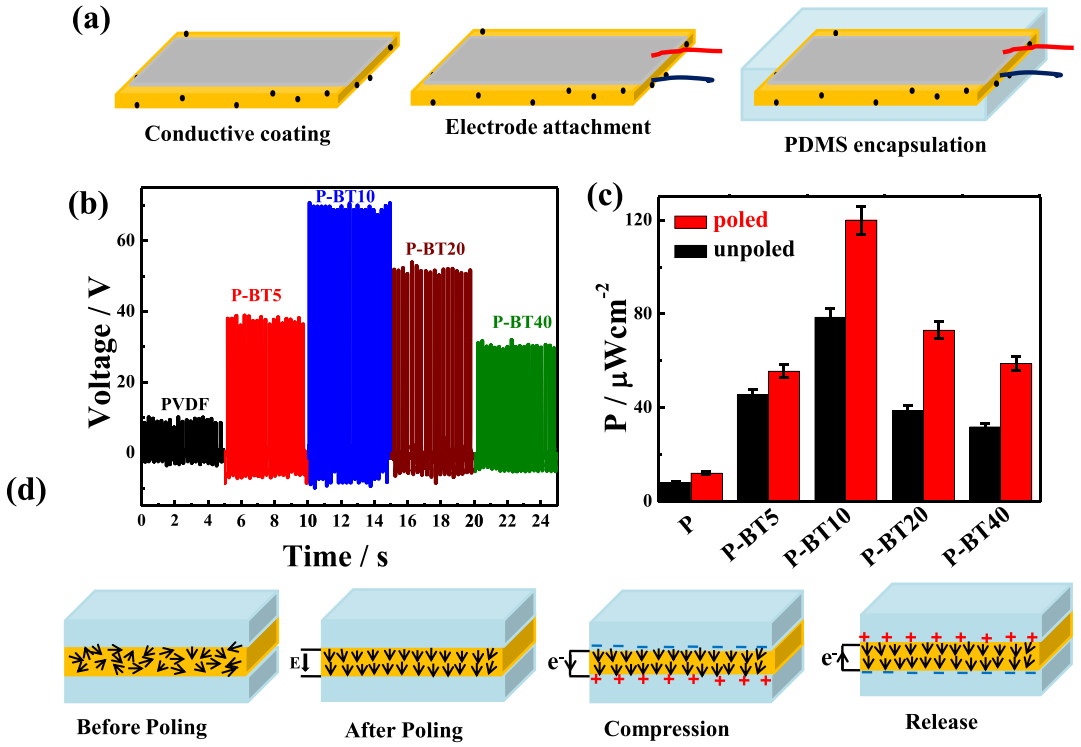

Figure 3. (a) Schematic of device preparation, (b) open circuit voltage of poled samples with different BT concentrations, (c) bar diagram showing power density of unpoled and poled samples with different BT contents, and (d) schematic of effect of poling and working principle of charge generation on the device.

to the stretching mode of O−H group, and the band at 1626 cm^{-1} is the bending mode of H−O−H, resulting from the physically absorbed water on BT nanoparticles (Figure S1). The characteristic absorption at 1443 cm^{-1} is stretching vibration of carboxylate because small amount of $BaCO_3$ is left in the sample. The FTIR plots for pure PVDF and nanocomposite (P-BT10) show that there is no structural changes after addition of the BT nanoparticles, that is, the nanocomposite is in the α-phase, but there is slight shifting in the peaks of nanocomposite, as shown, which shows the interaction between the nanoparticles and the PVDF. Figure 1c shows thermal behavior of the BT, PVDF, and their representative nanocomposite. The thermal degradation of pure PVDF and nanocomposite shows the single-step degradation in all the cases. There is no weight loss around 100 °C in the nanocomposites, which shows their hydrophobic nature. Both the PVDF and nanocomposites are stable up to 420 °C, and after this temperature, there is sudden loss of weight because of cleavage in polymer chains, arising from thermal degradation.[28] However, there is no change of degradation temperature in the composite as compared to pure PVDF. This is to mention that BT does not lose any weight up to 700 °C other than meager quantity of adsorbed water.

The DSC studies have also been done (Figure S2) and found that the increasing amount of BT nanoparticles does not affect the phase of polymer, as melting peaks of α-phases are observed in their melting endotherm; however, there is slight depression in the melting point from 173.79, 173.27, and 172.96 °C for PVDF, P-BT5, and P-BT20, respectively, which is because of the interaction between the PVDF and BT nanoparticles. The enthalpy of pure PVDF and nanocomposites is 39.8, 39.0, and 33.4 J/gm for P, P-BT5, and P-BT20, respectively. The slight reduction in enthalpy suggests good interaction between PVDF and BT. Thermal behavior and no change of structure have also been reported in previous work.[29]

The inclusion of nanoparticles changes its morphology of PVDF. Polarized optical microscopic images of pure PVDF, BT nanoparticles, and representative nanocomposite (P-BT10) are shown in Figure 2a. Pure PVDF shows the spherulitic pattern, which is because of its crystalline phase (α-phase).[30,31] The proper dispersion of nanoparticles can be seen in the nanocomposite (P-BT10). Further, the spherulites diameter drastically decreases in the presence of BT, indicating the nucleating nature of the BT particle. With higher percentage of BT, the agglomeration of nanoparticles takes place, which affects the performance of nanocomposite. The similar type of morphology is also confirmed through SEM images (Figure 2b), which clearly shows the spherulites in pure PVDF. Particulates of BT are clearly observed in the composite, showing its good dispersion in the PVDF matrix. The SEM image indicates the size of BT nanoparticles ∼130 nm, and XRD also confirms the crystallite size of ∼150 nm in its crystalline phase.

3.2. Device Performances and Applications. Barium titanate is piezoelectric in nature but it is brittle and not mechanically stable. Inclusion of BT nanoparticles in the PVDF matrix should be able to transform the nanocomposites into piezoelectric. The nanocomposites are flexible and highly stable under mechanical load. The energy-harvesting capability of the nanocomposites is evaluated by fabricating nanogenerators. The steps of device preparation are shown in Figure 3a, which illustrate the conductive coating, electrode attachment, and PDMS encapsulation of the device. For output voltage, measurements under impact load on the device

https://dx.doi.org/10.1021/acs.energyfuels.0c01143
Energy Fuels 2020, 34, 6239−6244

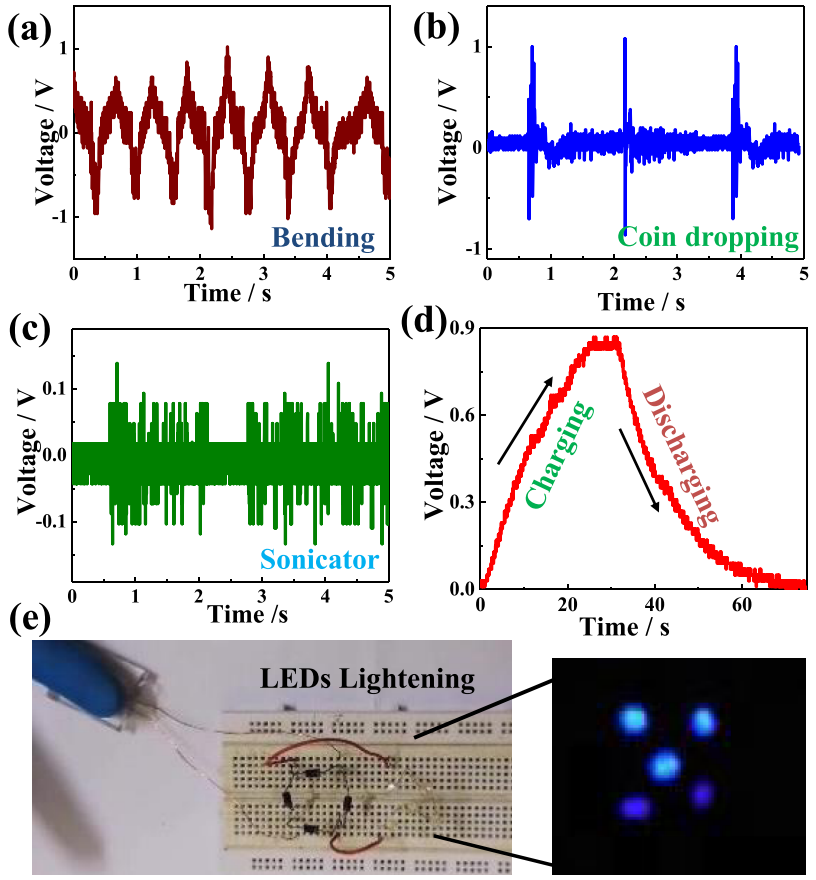

Figure 4. Practical applications of the device showing open circuit voltage from the device (a) on bending, (b) on coin dropping, (c) by ultrasonicator vibrations, (d) capacitor charging and discharging using the device by finger tapping, and (e) glowing of LED by finger tapping and corresponding circuit.

are performed using finger tapping, and the output voltage is measured using the oscilloscope. Pure PVDF shows only 5 V while nanocomposites with 5, 10, 20, and 40 wt % BT containing nanocomposites show 32, 66, 42, and 27 V, respectively (Figure S3). The nanocomposite with 10 wt % BT (P-BT10) shows the highest voltage output (66 V) while output voltage decreases at higher percentage of BT in the nanocomposites. The decrease in output may be because of the agglomeration of nanoparticles at higher percentage arising from cohesive force of BT particle.

To further enhance the output from the devices, poling has been performed at an electric field of 300 kV/cm for 1 h. The poled samples show enhanced voltage outputs from all the samples. Pure PVDF, P-BT5, P-BT10, P-B20, and P-BT40 exhibit the voltage output of 10, 45, 78, 58, and 35 V, respectively (Figure 3b). The device made from pure BT gives an output voltage of 100 V (Figure S4) after poling, which is very high and uniform as compared to the nonpoled sample, but the device is not stable and breaks upon repeated loading of stress. The energy-harvesting capability of the device is measured by its power output, which is calculated following the equation

$$P = \frac{V^2}{R \times A}$$

where V is the open circuit voltage measured across the resistance R, and A is the area of the device. Figure 3c shows the output power of poled and unpoled samples. The significant enhancement in output power is observed after poling as compared to unpoled samples. However, very high power density of ∼120 μW/cm^2 is observed using the composite of BT (10 wt %) and PVDF. The schematic in Figure 3d shows the poling and charge separation mechanism under stress, which causes this flow of output voltage in the circuit. The poling process aligns the dipoles in the nanocomposite, which improves its charge separation capability, presumably because of better dispersion of piezoparticulate, which, in turn, leads to increase in the output voltage. The poling is done under elevated temperature while applying the electric field across the samples. The barium titanate particles have dipoles, which try to orient themselves in the direction of electric field. The elevated temperature makes it easy to rotate the dipole within the particle. Therefore, the output from the poled samples, which have oriented dipoles, is more than the unpoled samples, which have random dipoles. On the application of stress, there is orientation of dipoles in the material, and this orientation of dipoles created the potential difference, which results in the electron flow in one direction while the electron flow in the reverse direction upon releasing the stress causes alternating current in the circuit.[32]

The prepared device can also be used in different practical applications as they can produce the voltage under various loading conditions, which can use the human body movement for energy harvesting. Some examples of these are shown in Figure 4. Figure 4a shows the open circuit voltage from the device upon repeated bending, which gives a voltage output of

https://dx.doi.org/10.1021/acs.energyfuels.0c01143
Energy Fuels 2020, 34, 6239−6244

2.2 V. Figure 4b shows the output voltage when 5 rupees coin is dropped on the device, which shows the output voltage of 1.8 V. Figure 4c shows the open circuit voltage using the sonicator vibrations, which is around 0.2 V (peak to peak). The charging and discharging of the 1 μF capacitor (Figure 4d) using finger tapping on the device is recorded, which shows that the capacitor charging takes ~30 s for charging up to 0.8 V. The device is also able to light up several LEDs by finger tapping. Figure 4e shows the lightning of the LEDs and corresponding circuit diagram. However, the developed device is able to generate the significant electrical signal, utilizing the waste mechanical resources, and act as the excellent energy-harvesting device, which is mechanically and thermally stable for practical applications.

4. CONCLUSIONS

The flexible nanocomposites of PVDF and BT nanoparticles have been prepared through the solution route. The structural studies show the proper inclusion of BT nanoparticles in the PVDF matrix. The morphological changes in the nanocomposites also demonstrate the good distribution of BT nanoparticles in the PVDF matrix. The device is fabricated to measure the output voltage from the nanocomposites using the human body movement like finger tapping. The poling process is used to enhance the output from the device as it arranges the dipoles in the material and enhances its charge separation capability, which leads to better output voltage. The highest open circuit voltage is obtained from the poled nanocomposite (with 10 wt % BT content) of 78 V and a power density of 120 μW/cm^2. The practical applications of the device are shown by producing voltage on different loading conditions, capacitor charging/discharging, and LED lightning. The prepared nanocomposite is piezoelectric in nature, and the device has potential to harvest energy on the basis of its piezoelectric properties. Thus, the flexible nanocomposite is able to harvest energy efficiently from mechanical and human body motions and is promising for a variety of applications in self-powered and independent systems.

■ ASSOCIATED CONTENT

Supporting Information

The Supporting Information is available free of charge at https://pubs.acs.org/doi/10.1021/acs.energyfuels.0c01143.

FTIR plot for pure BT nanoparticles, DSC curves for pure PVDF and nanocomposites, open circuit voltage of devices made of pure PVDF and different nanocomposites before poling, and open circuit voltage of pure barium titanate before and after poling (PDF)

■ AUTHOR INFORMATION

Corresponding Author

Pralay Maiti − *School of Materials Science and Technology, Indian Institute of Technology (Banaras Hindu University), Varanasi 221005, India;* orcid.org/0000-0002-6879-3591; Email: pmaiti.mst@itbhu.ac.in

Authors

Anupama Gaur − *School of Materials Science and Technology, Indian Institute of Technology (Banaras Hindu University), Varanasi 221005, India*

Shivam Tiwari − *School of Materials Science and Technology, Indian Institute of Technology (Banaras Hindu University), Varanasi 221005, India;* orcid.org/0000-0002-9210-5955

Chandan Kumar − *School of Biomedical Engineering, Indian Institute of Technology (Banaras Hindu University), Varanasi 221005, India*

Complete contact information is available at: https://pubs.acs.org/10.1021/acs.energyfuels.0c01143

Notes

The authors declare no competing financial interest.

■ ACKNOWLEDGMENTS

The author acknowledges Institute for her (A.G.) Teaching Assistantship.

■ REFERENCES

(1) Dakua, I.; Afzulpurkar, N. Piezoelectric energy generation and harvesting at the nano-scale: materials and devices. *Nanomater. Nanotechnol.* **2013**, *3*, 21.

(2) Anton, S. R.; Sodano, H. A. A review of power harvesting using piezoelectric materials (2003-2006). *Smart Mater. Struct.* **2007**, *16*, R1.

(3) Rocha, J. G.; Goncalves, L. M.; Rocha, P. F.; Silva, M. P.; Lanceros-Mendez, S. Energy harvesting from piezoelectric materials fully integrated in footwear. *IRE Trans. Ind. Electron.* **2009**, *57*, 813−819.

(4) Lee, C. S.; Joo, J.; Han, S.; Koh, S. K. Multifunctional transducer using poly (vinylidene fluoride) active layerand highly conducting poly (3,4-ethylenedioxythiophene) electrode: Actuator and generator. *Appl. Phys. Lett.* **2004**, *85*, 1841−1843.

(5) Lee, C. S.; Joo, J.; Han, S.; Lee, J. H.; Koh, S. K. Poly (vinylidene fluoride) transducers with highly conducting poly (3,4-ethylenedioxythiophene) electrodes. *Synth. Met.* **2005**, *152*, 49−52.

(6) Hadimani, R. L.; Bayramol, D. V.; Sion, N.; Shah, T.; Qian, L.; Shi, S.; Siores, E. Continuous production of piezoelectric PVDF fibre for e-textile applications. *Smart Mater. Struct.* **2013**, *22*, 075017.

(7) Qi, Y.; McAlpine, M. C. Nanotechnology-enabled flexible and biocompatible energy harvesting. *Energy Environ. Sci.* **2010**, *3*, 1275−1285.

(8) Reis, J.; Frias, C.; Canto e Castro, C.; Botelho, M. L.; Marques, A. T.; Simões, J. A. O.; Potes, J. A new piezoelectric actuator induces bone formation in vivo: a preliminary study. *BioMed Res. Int.* **2012**, *2012*, 613403.

(9) Wankhade, S. H.; Tiwari, S.; Gaur, A.; Maiti, P. PVDF-PZT nanohybrid based nanogenerator for energy harvesting applications. *Energy Rep.* **2020**, *6*, 358−364.

(10) Gaur, A.; Rana, D.; Maiti, P. Mechanical and wear behaviour of poly(vinylidene fluoride)/clay nanocomposite. *J. Mater. Res. Technol.* **2019**, *8*, 5874−5881.

(11) Jana, K. K.; Charan, C.; Shahi, V. K.; Mitra, K.; Ray, B.; Rana, D.; Maiti, P. Functionalized poly(vinylidene fluoride) nanohybrid for superior fuel cell membrane. *J. Membr. Sci.* **2015**, *481*, 124−136.

(12) Saxena, D.; Jana, K. K.; Soundararajan, N.; Katiyar, V.; Rana, D.; Maiti, P. Potency of nanolay on structural, mechanical and gas barrier properties of poly (ethylene terephthalate) Nanohybrid. *J. Polym. Res.* **2020**, *27*, 35.

(13) Saxena, D.; Soundararajan, N.; Katiyar, V.; Rana, D.; Maiti, P. Structural, mechanical, and gas barrier properties of poly(ethylene terephthalate) nanohybrid using nanotalc. *J. Appl. Polym. Sci.* **2019**, *137*, 48607.

(14) Saxena, D.; Rana, D.; Gowd, E. B.; Maiti, P. Improvement in mechanical and structural properties of poly (ethylene terephthalate) nanohybrid. *SN Appl. Sci.* **2019**, *1*, 1363.

(15) Saito, Y.; Takao, H.; Tani, T.; Nonoyama, T.; Takatori, K.; Homma, T.; Nagaya, T.; Nakamura, M. Lead-free piezoceramics. *Nature* **2004**, *432*, 84.

(16) Scott, J. F. Applications of modern ferroelectrics. *science* **2007**, *315*, 954−959.
(17) Aksel, E.; Jones, J. L. Advances in lead-free piezoelectric materials for sensors and actuators. *Sensors* **2010**, *10*, 1935−1954.
(18) Ning, L.; Liyuan, Y.; Jirui, D.; Xugui, P. Heavy metal pollution in surface water of Linglong gold mining area, China. *Procedia Environ. Sci.* **2011**, *10*, 914−917.
(19) García-Gutiérrez, M.-C.; Linares, A.; Hernández, J. J.; Rueda, D. R.; Ezquerra, T. A.; Poza, P.; Davies, R. J. Confinement-induced one-dimensional ferroelectric polymer arrays. *Nano Lett.* **2010**, *10*, 1472−1476.
(20) Saravanakumar, B.; Soyoon, S.; Kim, S.-J. Self-Powered pH Sensor Based on a Flexible Organic-Inorganic Hybrid Composite Nanogenerator. *ACS Appl. Mater. Interfaces* **2014**, *6*, 13716−13723.
(21) Lee, C.; Wood, D.; Edmondson, D.; Yao, D.; Erickson, A. E.; Tsao, C. T.; Revia, R. A.; Kim, H.; Zhang, M. Electrospun uniaxially-aligned composite nanofibers as highly-efficient piezoelectric material. *Ceram. Int.* **2016**, *42*, 2734−2740.
(22) Lin, Z.-H.; Yang, Y.; Wu, J. M.; Liu, Y.; Zhang, F.; Wang, Z. L. BaTiO3 nanotubes-based flexible and transparent nanogenerators. *J. Phys. Chem. Lett.* **2012**, *3*, 3599−3604.
(23) Park, K.-I.; Lee, M.; Liu, Y.; Moon, S.; Hwang, G.-T.; Zhu, G.; Kim, J. E.; Kim, S. O.; Kim, D. K.; Wang, Z. L.; Lee, K. J. Flexible nanocomposite generator made of BaTiO3 nanoparticles and graphitic carbons. *Adv. Mater.* **2012**, *24*, 2999−3004.
(24) Buscaglia, M. T.; Bassoli, M.; Buscaglia, V.; Alessio, R. Solid-State Synthesis of Ultrafine BaTiO3 Powders from Nanocrystalline BaCO3 and TiO2. *J. Am. Ceram. Soc.* **2005**, *88*, 2374−2379.
(25) Edmondson, D.; Cooper, A.; Jana, S.; Wood, D.; Zhang, M. Centrifugal electrospinning of highly aligned polymer nanofibers over a large area. *J. Mater. Chem.* **2012**, *22*, 18646−18652.
(26) Ramajo, L.; Castro, M. S.; Reboredo, M. M. Effect of silane as coupling agent on the dielectric properties of BaTiO3-epoxy composites. *Composites, Part A* **2007**, *38*, 1852−1859.
(27) Chang, S.-J.; Liao, W.-S.; Ciou, C.-J.; Lee, J.-T.; Li, C.-C. An efficient approach to derive hydroxyl groups on the surface of barium titanate nanoparticles to improve its chemical modification ability. *J. Colloid Interface Sci.* **2009**, *329*, 300−305.
(28) Revathi, S.; Kennedy, L. J.; Basha, S. K. K.; Padmanabhan, R. Synthesis, Structural, Optical and Dielectric Properties of Nano-structured 0-3 PZT/PVDF Composite Films. *J. Nanosci. Nanotechnol.* **2018**, *18*, 4953−4962.
(29) Nunes-Pereira, J.; Sencadas, V.; Correia, V.; Rocha, J. G.; Lanceros-Méndez, S. Energy harvesting performance of piezoelectric electrospun polymer fibers and polymer/ceramic composites. *Sens. Actuators, A* **2013**, *196*, 55−62.
(30) Gaur, A.; Kumar, C.; Shukla, R.; Maiti, P. Induced Piezoelectricity in Poly(vinylidene fluoride) Hybrid as Efficient Energy Harvester. *ChemistrySelect* **2017**, *2*, 8278−8287.
(31) Gaur, A.; Kumar, C.; Tiwari, S.; Maiti, P. Efficient Energy Harvesting Using Processed Poly(vinylidene fluoride) Nanogenerator. *ACS Appl. Energy Mater.* **2018**, *1*, 3019−3024.
(32) Lee, J.-H.; Yoon, H.-J.; Kim, T. Y.; Gupta, M. K.; Lee, J. H.; Seung, W.; Ryu, H.; Kim, S.-W. Micropatterned P(VDF-TrFE) Film-Based Piezoelectric Nanogenerators for Highly Sensitive Self-Powered Pressure Sensors. *Adv. Funct. Mater.* **2015**, *25*, 3203−3209.

https://dx.doi.org/10.1021/acs.energyfuels.0c01143
Energy Fuels 2020, 34, 6239−6244